Revised to Atmospheirc Environment Special Issue

Springtime variations of organic and inorganic constituents in submicron aerosols ($PM_{1.0}$) from Cape Hedo, Okinawa

Bhagawati Kunwar[1], K. Torii[1,2], C. Zhu[1], Pingqing Fu[1,3] and Kimitaka Kawamura[1*]

[1]Institute of Low Temperature Science, Hokkaido University, N19 W8, Kita-ku, Sapporo, Japan

[2]Graduate School of Environmental Science, Hokkaido University, N11 W5, Kita-ku, Sapporo, Japan

[3]State Key Laboratory of Atmospheric Boundary Layer Physics and Atmospheric Chemistry, Institute of Atmospheric Physics, Chinese Academy of Sciences, Beijing 100029, China

[*]Corresponding author (email: kawamura@lowtem.hokudai.ac.jp)

Abstract

During the spring season with enhanced Asian outflow, we collected submicron aerosol ($PM_{1.0}$) samples at Cape Hedo, Okinawa Island in the western North Pacific Rim. We analyzed the filter samples for diacids, oxoacids, pyruvic acid, α-dicarbonyls and fatty acids to better understand the sources and atmospheric processes in the outflow regions of Asian pollutants. Molecular distributions of diacids show a predominance of oxalic acid (C_2) followed by malonic (C_3) and succinic (C_4) acids. Total diacids strongly correlated with secondary source tracers such as SO_4^{2-} (r=0.87), NH_4^+ (0.90) and methanesulfonate (MSA^-) (0.84), suggesting that diacids are secondarily formed from their precursor compounds. We also found good correlations among C_2, organic carbon (OC) and elemental carbon (EC) in the Okinawa aerosols, suggesting that diacids are mainly derived from anthropogenic sources. However, a weak correlation of diacids with levoglucosan, a biomass burning tracer, suggests that biomass buring is not the main source of diacids, rather diacids are secondarily formed by photochemical oxidation of organic precursors derived from fossil fuel combustion. We found a strong correlation (r = 0.98) between inorganic nitrogen (NO_3-N + NH_4-N) and total nitrogen (TN), to which organic nitrogen (ON) contributed 23%. Fatty acids were characterized by even carbon number predominance, suggesting that they are derived from biogenic sources. The higher abundances of short chain fatty acids ($<C_{20}$) than long chain fatty acids ($>C_{20}$) further suggest that fatty acids are largely derived from marine phytoplankton during spring bloom.

Keywords: submicron aerosols, diacids and related compounds, organic nitrogen, Okinawa, atmospheric aging

1. Introduction

Atmospheric aerosols are generally enriched with water-soluble oraganic (dominated by oxalic acid) and inorganic (sulfate) components (e.g., Jimnetz et al., 2009; Kawamura et al., 2010). Those atmospheric particles have an impact on the Earth's radiative balance and hydrological cycles (Ramanathan et al., 2001) as well as adverse health effect to the human pulmonary tract (Mitchell et al., 1987). The extent of such impacts largely depends upon the chemical composition of atmospheric aerosols. Aerosols are emitted from the various primarily sources such as soil dust, fossil fuel combustion, vehicular and biomass burning emission, and sea salt via the sea spray. They are also secondarily formed via the atmospheric oxidation of inorganic and organic precursors in the presence of sunlight and oxidants. Primary and secondary aerosols together with their atmospheric circulations have an influence on local to regional air quality, atmospheric loadings and chemical compositions (Pavuluri et al., 2015). Based upon the model study, organic aerosols are known to be largely subjected to chemical transformation (Kanakidou et al., 2005).

In East Asia, emissions of pollutants (both organic and inorganic) are increasing due to the growing activities of Chinese industries and biomass burning in Southeast and East Asia (Kunwar and Kawamura, 2014; Zhu et al., 2015). The anthropogenic emissions in East Asia are much more severe than any other regions in the world and this situation will continue to increase for the coming decades (Ohara et al., 2007). For example, the pollutants emitted from China are recognized to have a significant impact on the air quality in the outflow regions, such as Okinawa Island in the western North Pacific Rim, by long range atmospheric transport (Kunwar and Kawamura, 2014a). Similarly, major sources of organic nitrogen in the atmosphere include vehicle exhaust, landfill, marine biological algal blooms and bacteria, dust and biomass burning (Westerholm et al., 1993; Kallinger and Niessner,

1999; Wedyan and Preston, 2008; Timperley et al., 1985). Wang et al. (2013) reported the abundant presence of water soluble organic nitrogen (WSON) in Chinese aerosols.

In a previous study, we reported the seasonal variations of organic and inorganic aerosols in the TSP samples from Cape Hedo, Okinawa (Kunwar and Kawamura, 2014a, b). However, there are no studies of diacids together with organic nitrogen and related compounds in $PM_{1.0}$ filter samples in marine aerosols in the Asian outflow region, although there are many studies on total suspended particles (Fu et al., 2013 and references therein; Kundu et al., 2010; Wang et al., 2006; Kawamura and Sakaguchi,1999). Cape Hedo is situated on the northwestern edge of Okinawa Island, Japan, an outflow region of East Asian pollutants. Around the sampling location, there is no major anthropogenic activity (Yamamoto et al., 2011) and thus Cape Hedo has been used as a supersite of Atmospheric Brown Cloud (ABC) project to study the East Asian aerosols (Takami et al., 2007).

In this study, we report the day-by-day variations of diacids, oxoacids, α-dicarbonyls and benzoic acid, and fatty acids, together with organic carbon, elemental carbon, major ions and organic nitrogen in $PM_{1.0}$ samples from Cape Hedo. To better understand the sources and atmospheric processing of organic aerosols at Cape Hedo, we compare the data of diacids and related compounds together with inorganic ions and a biomass buring tracer, i.e., levoglucosan, a specific pyrolysis product of cellulose and hemicellulose (Simoneit, 1999).

2. Samples and analytical procedure

2.1. Site description and aerosol sampling

Aerosol sample collection was performed at the rooftop of the facility of Cape Hedo Atmosphere and Aerosol Measurement Station (CHAAMS, 26º 9´ N, 128° 2´ E) during 17 March to 13 April, 2008. Figure 1 shows a map of Okinawa along with East Asia and the Pacific Ocean. $PM_{1.0}$ samples (n=28) were collected at CHAAMS station using low volume

air sampler and pre-combusted (450°C, 4 hours) quartz fiber filters (Pallflex 2500QAT, 47 mm in diameter). The flow rate was 16.7 l/min. Blank filters (n=4) were collected every week. Each sample was collected for 24 hours. Before and after sampling, the filters were stored in a preheated glass vial (50 mL) with a Teflon-lined screw cap. The samples were stored in darkness at −20°C until the analysis. During the sampling period, average temperature and relative humidity were 19.7°C and 71%, respectively. The weather conditions were cloudy and fine during the campaign, but there were rainfall events in March 18 and 30 and April 13. The ambient temperature, rainfall, and relative humidity are shown in Figure S2.

2.3. Chemical analysis

Filter samples were analysed for water-soluble diacids, oxoacids, and α-dicarbonyls by the method reported previously (Kawamura and Ikushima, 1993; Kawamura, 1993). Known area of filter was extracted with organic-free pure water and then carboxylic acids and α-dicarbonyls in the extracts were derivatized with 14% BF_3/n-butanol to butyl esters and/or dibutoxy acetals. The derivatives were determined using a capillary gas chromatography (GC; HP 6890). The GC peaks were identified by comparing the GC retention times with those of authentic standards and the peak identifications were confirmed by mass spectral examination using a GC/mass spectrometry (GC/MS) system. Both field and laboratory blanks were analyzed. Oxalic acid and other organic species were detected in the blanks. However, their concentrations were less than 5% of the real samples. The concentrations of all species reported here are corrected for blanks. We also performed the recovery test by spiking authentic dicarboxylic acids to the quartz filter. The recoveries of spiked diacids were 94% for oxalic acid (C_2) and more than 97% for C_3, C_4, C_5 and C_6 diacids. The reproducibility in the measurements of major diacids (C_2, C_3, and C_4) was ca. 10%.

For the determination of levoglucosan, a small punch of each filter was extracted with dichloromethane/methanol (2:1, v/v) under ultrasonication. The extracts were concentrated using a rotary ecaporator, and then reacted with N,O-bis-(trimethylsilyl)trifluoroacetamide (BSTFA) to derive TMS ethers of levoglucosan. Levoglucosan was measured by gas chromatography/mass spectrometry (GC/MS). Detailed analytical procedures can be found elsewhere (Fu et al., 2012).

To measure total nitrogen (TN), we combusted a small filter disc placed in a tin cup at 1400°C using elemental analyzer (EA) (Thermo Scientific, Trace GC Ultra, Delta V Advantage Isotope Ratio MS). All the nitrogen species are converted to NO and further reduced to N_2 in a reduction column. N_2 is separated on a packed column of gas chromatograph installed in EA and measured with a thermal conductivity detector. Organic nitrogen (ON) is calculated using following equation.

$$ON = TN - IN$$

where IN (inorganic nitrogen) means the summation of nitrate (NO_3^-) and ammonium (NH_4^+) nitrogen. NO_3^-, NH_4^+ and other major ions were determined using an ion chromatograph (761 Compact IC, Metrohm, Switzerland). Details of analytical procedures for ions are reported in Kunwar and Kawamura (2014a).

Organic carbon (OC) and elemental carbon (EC) were measured using a Sunset Laboratory carbon (OC/EC) analyzer following Integragency Monitoring Protected Visual Environments (IMPROVE) thermal/optical evolution protocol. Detailed procecure is described in Kunwar and Kawamura (2014a).

2.4. Air Mass backward trajectory analysis and fire counts

Figure 1a shows the 5-day back trajectories above the 500 meter for every day using the Hybrid Single-Particle Lagrangian Integrated Trajectory (HYSPLIT4) model (Draxler

and Hess, 1998). Except for few days, air masses in the study area were transported from East Asia. During March 17 and 18 and April 6 and 9, air masses were delivered from the Pacific Ocean over the sampling site. Figure 1b shows the fire counts in East Asia obtained by satellite (https://earthdata.nasa.gov/data/near-real-time-data/firms/active-fire-data) with 5-day back trajectories.

3. Results and Discussion

3.1. Molecular distributions of dicarboxylic acids, oxoacids and α-dicarbonyls

We detected homologous series of α,ω-dicarboxylic acids (C_2-C_{12}), unsaturated diacids (phthalic, isophthalic, terephthalic, maleic, fumaric and methylmaleic), multi-functional diacids (malic, ketomalonic, and 4-ketopimelic), oxocarboxylic acids (ωC_2-ωC_9 and pyruvic acid), α-dicarbonyls (glyoxal and methylglyoxal) and benzoic acid in the $PM_{1.0}$ samples. In addition, we also detected homologous series of fatty acids. Figure 2 shows the average molecular distribution of diacids, oxoacids and α-dicarbonyls.

Concentrations of total diacids, oxoacids and α-dicarbonyls ranged from 114-537 ng m^{-3} (av., 273±121 ng m^{-3}), 5.5-53 ng m^{-3} (27±15 ng m^{-3}), and 2.9-19 ng m^{-3} (7.8±4.2 ng m^{-3}), respectively (Table 1). Oxalic acid (C_2) was found as the most abundant species followed by malonic (C_3), succinic (C_4), glyoxylic (ωC_2), ketomalonic (kC_3) and phthalic (Ph) acid. The molecular distributions of diacids in the Cape Hedo aerosols are similar to those reported from Gosan site, Jeju Island, South Korea (C_2>C_3>C_4) (Kundu et al., 2010). The predominance of ωC_2 and kC_3 after C_2 to C_4 indicates a significant photochemical processing during long range transport. Both ωC_2 and kC_3 are the precursors of C_2 (Kawamura et al., 1996). The highest relative abundance of C_2 in total C_2-C_{12} (78%) was observed in April 13, whereas the lowest value (55%) was observed in March 20.

159 **3.2. Temporal variations of diacids, oxoacids and α-dicarbonyls**

160 Figure 3 shows temporal variations of diacids, oxoacids and α-dicarbonyls. Except for
161 azelaic acid (C_9), short chain diacids (C_2 to C_6) present similar temporal variations. The
162 temporal variations suggest that the source and/or formation process of diacids are similar
163 except for C_9. Oxalic acid shows the highest concentration in April 3, whereas the lowest
164 concentration was observed in March 18 (Figure 3a). Back trajectory analysis revealed that
165 air masses of April 3 originated from Mongolia passing over the northern part of China
166 whereas the air masses of April 18 were delivered from the Pacific Ocean. The temporal
167 variations of C_3 and C_4 are similar with that of C_2. Interestingly, C_3 and C_4 peaked on April 8
168 (Figure 3b and 3c). On the same date, 9-oxononanoic acid (ωC_9), an oxidation product of
169 unsaturated fatty acids (Kawamura and Gagosian, 1987), maximized (Figure 3i). The
170 different temporal variation between ωC_9 and C_9 is due to the presence of active –CHO group
171 in ωC_9 that makes ωC_9 more reactive and semi-volatile. The air masses of April 8 originated
172 from South Asia. These results suggest that unsaturated fatty acids are oxidized to result in C_3
173 and C_4 diacids as well as ωC_9 during the long range transport from South Asia.

174 Adipid acid (C_6), a tracer of anthropogenic sources (Kawamura and Ikushima, 1993),
175 showed the highest concentration in April 10 followed by April 3 whereas the lowest
176 concentration was found in April 13. Although air masses originated from the Pacific Ocean
177 passing over the Japanese Islands, the air parcels were encounted with rainfall around Cape
178 Hedo in April 13 and thus the concentration was declined. During April 10 and April 5, air
179 masses from East Asia were delivered to Cape Hedo with air pollutants. Phthalic acid (Ph), a
180 tracer of anthropogenic source (Kawamura and Ikushima, 1993), also showed the highest
181 concentration in April 5 (Figure 3f), whereas the lowest concentration was found in April 6,
182 one day before a small rain event was recorded in Okinawa.

Terephthalic acid (tPh) has been proposed as an organic tracer of plastic burning (Kawamura and Pavuluri, 2010; Pavuluri et al., 2010; Simoneit et al., 2005). This tracer maximized in April 3 (not shown as a figure). Azelaic acid (C_9), a tracer for the oxidation of biogenic unsaturated fatty acids such as $C_{18:1}$ (Kawamura and Gagosian, 1987), peaked in April 3 (Figure 3e), whereas lower concentration was found in April 7 although the air mass source region is East Asia. C_9 is the first oxidation product of unsaturated fatty acids emitted from biogenic sources, biomass burning of plants, meat cooking operation and plant leaf abrasion (e.g., Ho et al., 2010). Glyoxylic acid (ωC_2), which is a precursor of C_2 and is formed by the oxidation of aromatic hydrocarbans such as benzene and toluene, showed the highest concentration in April 3. The peaks of C_2 and ωC_2 in April 3 suggest a significant oxidation of precursor compounds. Both glyoxal (Gly) and methylglyoxal (MeGly) show higher concentrations in April 1. The temporal variation of ωC_2 is similar to C_2 whereas that of ωC_4 is similar to C_4. These results suggest that C_2 and C_4 are formed by the oxidation of corresponding oxoacids (ωC_2 and ωC_4). The temporal variations of Gly and MeGly are similar to that of C_2, suggesting that C_2 may be the oxidation product of α-dicarbonyls.

Benzoic acid has been proposed as a primary pollutant emitted from vehicular exhaust (Kawamura et al., 1985; Ho et al., 2006) and secondary photochemical oxidation of aromatic hydrocarbons such as toluene from automobiles (Suh et al., 2003). Very high ambient levels of toluene (11.4 $\mu g\ m^{-3}$) were detected in Beijing (Duan et al., 2008). Guo et al. (2004) reported daily concentration of toluene up to 50 $\mu g\ m^{-3}$ in Hong Kong. Higher concentrations of benzoic acid were recorded in March 20, 28 and 29, and April 3 and 8 in Cape Hedo. The high abundance of benzoic acid in this study suggests a signinificant contribution of toluene and subsequent oxidation during the long range atmospheric transport from the Asian Continent.

During the campaign, there were many but minor rainfall events in the study site (March 17, 18, 23 and 30, and April 3, 10 and 13), suggesting that these organic species were washed out from the atmosphere near the sampling site. In fact, during these rainy days, we found lower concentrations of diacids, oxoacids and α-dicarbonyls, except for April 3.

Malonic (C_3) to succinic (C_4) acid ratio has been used as an indicator of photochemical aging of organic aerosol (OA) (e.g., Kawamura and Ikushima, 1993). The C_3/C_4 ratios are higher in March 30 and April 6, whereas it was lowest in April 5. Except for the samples of March 30 and April 5 and 6, C_3/C_4 ratios do not show a significant variation, suggesting that Cape Hedo aerosols are photochemically more aged probably during long-range atmospheric transport. In fact, the air mass source regions associated with the high C_3/C_4 ratios are located in Northwest and Northeast China, from which polluted aerosols were transported long distances to the sampling site in Okinawa. The average C_3/C_4 ratio in this study is 1.3. Similar but higher ratio (1.7) was observed for TSP samples from the same site (Kunwar and Kawamura 2014b), the Southern Ocean (1.7) (Fu et al., 2013) and Western North Pacific (0.91 to 1.5) (Fu et al., 2013). Average C_3/C_4 ratio in this study is lower than those from the Indian Ocean (2.1) (Fu et al., 2013), South China Sea (2.7) (Fu et al., 2013) and Pacific Ocean (4) (Kawamura and Sakaguchi, 1999), suggesting that photochemical aging of Okinawa aerosols are less significant than the open ocean aerosols.

C_6 and Ph acids are produced by the oxidation of anthropogenic cyclohexane and aromatic hydrocarbons, respectively (Kawamura and Ikushima, 1993), whereas C_9 is produced by the oxidation of biogenic unsaturated fatty acids having double bond at C9 position as stated above. Hence, C_6 to C_9 and Ph to C_9 ratios can be useful tracers to evaluate the relative contributions of anthropogenic and biogenic sources (Ho et al., 2006; Wang et al., 2009). Both C_6/C_9 and Ph/C_9 ratios peaked in April 7 (Figure 4). On this date, the air mass source regions are the coasts of China (Guangzhou, Shantou and Xiamen, not shown as a

figure). The lowest concentration of C_9 at this day is due to the difference in source region. Lower C_6/C_9 ratios were observed in March 18, 19, 23, 30, and April 5 and 13. Lower Ph/C_9 ratios were also observed in March 23 and 30. These results suggest that there are more biogenic contributions on those days. Spring is a growing season with more biogenic emissions. Maleic acid (M) can be isomerized to fumaric acid (F) under strong solar radiation during long range atmospheric transport. A significant photo-isomerization of M to F was observed in April 2 and 3 (Figure 4d) when air masses were delivered from North China and local temperature in Okinawa was not high (Figure S2). This result suggest that photo-isomerization is enhanced during long range atmospheric transport.

The average F/M ratio in this study is 0.43. This value is several times lower than that of the springtime TSP aerosols (1.9) from the same sampling site (Kunwar and Kawamura, 1014b), the South China Sea (1.9) (Fu et al., 2003), North Atlantic (2) (Fu et al., 2013), Indian Ocean (3.8) (Fu et al., 2013), and Western North Pacific (1.1) (Fu et al., 2013). These comparison suggests that larger particles may be photochemically more aged in the marine atmosphere during the accumulation and coagulation process of fine particules.

3.2. Carbonaceous components and organic nitrogen

Concentrations of organic carbon (OC) and elemental carbon (EC) ranged from 0.41 to 2.49 μg m^{-3} (av. 1.2 μg m^{-3}) and 0 to 0.85 (av. 0.36 μg m^{-3}), respectively. Higher concentrations of OC were observed in March 28 and April 3, whereas the lowest concentrations were observed in March 23 and April 6 (Figure 5a). Similarly, the highest concentration of EC was found in March 28, whereas the lowest value was observed in March 18. A strong correlation (r=0.82) between OC and EC (Figure 6a) during the whole campaign suggests that they have similar sources. OC to EC ratio is a useful tool to discuss the sources of aerosols (Kunwar and Kawamura 2014a). The OC/EC ratios > 2.0 indicate a significant contribution of secondary organic aerosol (SOA) (Cao et al., 2003). OC/EC ratios

in the study area are > 2, suggesting a significant fraction of OC in Cape Hedo aerosols is of SOA origin. The highest OC/EC ratio (12.7) was found in March 18 (not shown as a figure), which may be due to more biogenic emission of organic aerosols and precursors from marine sources and/or lower contributions of EC. Back trajectory analysis shows that air masses of March 18 were delivered from oceanic regions (Figure 1). We found similar temporal variations of total diacids with OC and EC. A strong correlation between OC with total diacids (r=0.84) suggests that diacids are mostly derived from anthropogenic sources from East Asia via long-range transport.

Concentrations of organic nitrogen (ON) ranged from 0.0 to 1.5 μg m^{-3} (av. 0.54 μg m^{-3}) (Figure 5b). The temporal variation of ON is similar to those of OC, NH_4^+ and nss-SO_4^{2-}, suggesting that source of ON is East Asia. There are various sources of organic nitrogen in the atmosphere; e.g., emission from vehicular exhaust (Westerholm et al., 1993) marine algal blooms and bacteria (Sorooshian et al., 2008), biomass burning, cooking (Simoneit et al., 2002), etc. Higher concentration of ON was observed in April 3, when air mass came from northern part of China. Contribution of ON to total nitrogen is 23%. We found higher percentage of ON for one year observation of TSP samples (37%) (unpublished data), suggesting that organic nitrogen is present in larger size fraction of aerosols. In fact, very high concentration of WSON have been reported in China during the dust storm event (Wang et al., 2013). We found higher contribution of NH_4-N to TN in $PM_{1.0}$ samples than TSP samples (unpublished data). The higher concentration of NO_3-N in coarse fraction suggests that NO_3^- is associated with coarse particles during long range atmospheric transport. We found strong correlation between IN and ON (r =0.98) (Figure 7), suggesting the similar sources of these nitrogenous compounds. We did not find statistically significant correlation between levoglucosan and ON, suggesting that ON is not emitted from the biomass burning

in this region. However, Mace et al. (2003) reported that organic nitrogen is emitted from biomss burning.

3.3. Temporal variation of anthropogenic tracers and evidence for secondary formation of diacids

nss-SO_4^{2-} can be used as an anthropogenic tracer of industrial origin and NH_4^+ is a tracer of biomass burning, agricultural wastes and animal excreta (Pavuluri et al., 2011). The temporal variations of NH_4^+ and SO_4^{2-} are similar (Figure 5c, 5d). Both nss-SO_4^{2-} and NH_4^+ show higher concentrations in March 29. A strong correlation (r=0.98) between nss-SO_4^{2-} and NH_4^+ supports a similar oxidation pathway to form NH_4HSO_4 or $(NH_4)_2SO_4$ (Figure 6b). nss-SO_4^{2-} and MSA^- are formed by the photochemical oxidation in the atmosphere.

Total diacids show strong correlations with NH_4^+ (r=0.90), nss-SO_4^{2-} (0.87) and MSA^- (0.84) (Figure 8a, b, c). MSA^- is formed by the oxidation of dimethyl sulfide (DMS) that is emitted from industrial emission (Yuan et al., 2004) although DMS is also emitted from the ocean by microbial activity (Saltzman et al., 1983). A strong correlation between MSA^- and total diacids suggests that diacids are mainly formed from the secondary formation from industrial emission. Yuan et al. (2004) reported significant concentrations of MSA^- in Beijing. Although Na^+ is emitted primarily from the ocean, we found a negative correlation (r=0.31) between Na^+ and diacids (Figure 8d), suggesting that diacids are not of marine origin. nss-Ca^{2+} is a major component of dust. In spring, our sampling site is influenced from dust emitted from the arid regions in East Asia (Kunwar and Kawamura, 2014a). Although nss-Ca^{2+} was not detect in the $PM_{1.0}$ samples, we found abundant nss-Ca^{2+} in TSP samples collected at the same site in spring (Kunwar and Kawamura, 2014a).

Levoglucosan is a specific sugar compound formed by the pyrolysis of cellulose at high temperature (>300°C) (Simoneit et al., 1999). Concentrations of levoglucosan ranged

from 0.43 to 8.1 ng m^{-3} (3.4±2.5 ng m^{-3}). Higher concentrations of levoglucosan were observed in March 20, 22, 28, and April1, 2, 3, 4 and April 10. nss-K^+ is another tracer for biomass burning, which showed co-varied peaks with levoglucosan (Figure 5g). However, we observed relatively weak correlation between the two tracers (r=0.44). We checked the back trajectory along with fire counts during March 20, 22 and 28, and April1 2, 3, 4, and 10. Except for March 28 and April 2, air masses were influenced from the areas with high fire counts, whereas during March 28 and April 2, air masses did not passed over the areas with high fire counts. This results may suggest that, in addition to open biomass burning, closed or domestic biomass burning is also important in East Asia (Sang et al., 2011 and references therein).

To better understand the sources and transformation process, we performed correlation analyses for selected diacids, oxoacids, inorganic ions, and levoglucosan (Table 2). We found that C_2 is strongly correlated with its precursor compounds such as C_3 (r=0.94), C_4 (0.90), ωC_2 (0.83), and pyr (0.73). These strong correlations suggest that the predominance of C_2 is involved with chain reactions of its precursors. The fair correlation (0.64) between C_2 and benzoic acid suggest that C_2 come in part from vehicular emission or atmospheric oxidation of aromatic hydrocarbons because benzoic acid is a tracer of vehicular emission (Ho et al., 2010; Kawamura and Kaplan, 1987) and is produced by the oxidation of of toluene (Suh et al., 2003). It is interesting to note that there is no correlation between C_9 and short chain (C_2-C_4) diacids, suggesting that small diacids are not derived from biological sources. We observed a weak correlation (r=0.46) between oxalic acid and levoglucosan, instead, correlations are strong among oxalic acid, NH_4^+ and nss-SO_4^{2-}, suggesting that the Okinawa aerosols are largely involved with the secondary formation with vigorous photochemical processing.

3.4. Possible sources of diacids and ionic species

To understand the possible sources of diacids and major ions, we performed principal component analysis using varimax rotation with Kaiser Normalization (SPSS software). As shown in Table 3, four components were found. C_2 to C_5, ωC_2, NH_4^+, MSA^- and $nssSO_4^{2-}$ show high loadings in Component 1. Component 1 is associated with anthropogenic sources followed by photochemical oxidation because $nss\text{-}SO_4^{2-}$, NH_4^+, MSA^- are emitted from anthropogenic sources including industrial emissions, biofuel burning, and animal excreta. ωC_2 is formed by the oxidation of aromatic hydrocarbons. Component 2 is associated with biogenic sources because C_7 and C_8 diacids are produced by photochemical oxidation of biogenic unsaturated fatty acids emitted from terrestrial higher plants and marine phytoplankton (Pavuluri et al., 2010). Higher loadings of C_9 and levoglucosan in Component 3 suggest that C_9 diacid is associated with biomass burning. High loadings of Na^+ and NO_3^- in Component 4 suggest the adsorbtion of HNO_3 on the surface of sea-salts (Deshmukh et al., 2013). These results suggest that springtime aerosols are largely influenced from industrial emission, terrestrial and marine biological emission, agricultural activity and biomass burning.

3.5. Molecular distributions of fatty acids

Figure 9 shows average molecular distribution of fatty acids. Short chain fatty acids ($\leq C_{19}$) are emitted from vascular plants, microbes, and marine phytoplankton, while long chain fatty acids ($\geq C_{20}$) are limited to terrestrial higher plant waxes (Kawamura et al., 2004; Simoneit, 1978; Kolattukudy, 1976). Average molecular distribution showed the peak of $C_{14:0}$ fatty acid followed by $C_{16:0}$ and $C_{18:0}$. The predominance of even carbon number fatty acids suggests an important contribution of biological sources to the Okinawa aerosols. $C_{18:1}$ is highly reactive compared to $C_{18:0}$ in the atmosphere due to the presence of double bond. Thus, the ratios of $C_{18:1}/C_{18:0}$ can be used to evaluate the aging process of organic aerosols (Ho et al., 2011). Very high ratios were observed in April 7 followed by April 10 and 9 whereas lower ratios were observed in March 31, April 1 and 2. The lower ratios are associated with

the photochemical oxidation process. The fresh organic aerosols were obtained in April 7 whereas the aged aerosols were obtained during March 31 and April 1. In April 7, air masses were delivered from the coastal region of China, whereas air masses of March 31 were delivered from Mongolia via North China and air masses of April 1 were originated from North China.

4. Summary and Conclusions

We measured dicarboxylic acids, oxoacids, α-dicarbonyls and benzoic acid as well as fatty acids in the springtime $PM_{1.0}$ aerosols from Cape Hedo, Okinawa to better understand the source and formation processes. Among diacids and related compounds, C_2 is most abundant species (172±73 ng m^{-3}) followed by C_3 (26±13 ng m^{-3}) and C_4 (21±11 ng m^{-3}). Molecular distribution of diacids suggests that they are formed by the photochemical oxidation of anthropogenic and biogenic precursors during long range atmospheric transport. Higher concentrations of C_2, C_6 and benzoic acid in the aerosols (April 3) suggest significant influences from anthropogenic activities including vehicular emission. Strong correlations between total diacids and EC suggest that diacids are mostly transported from the polluted regions of East Asia. We found a strong correlation between MSA^- and total diacids, suggesting that some fractions of diacids were derived with industrial emissions from Chinese megacities. Temporal variations of OC, EC, nss-SO_4^{2-}, NH_4^+ and ON are similar, suggesting that organic nitrogen is emitted from the anthropogenic sources in East Asia. No correlation between ON and levoglucosan suggests that ON is not emitted from biomass burning. The even carbon number predominance of short chain fatty acids ($<C_{20}$) further suggests that marine emission is also important source during the campaign.

Aknowledgement

380 This study was in part supported by the Japan Society for the Promotion of Science
381 (grant-in-aid No. 24221001) and the Environment Research and Technology Development
382 Fund (B-0903) from the Ministry of the Environment, Japan. We thank to Y. Kitamori and S.
383 Aggarwal for their helps during sample collection.We also thank the NOAA Air Resource
384 Laboratory (ARL) for the provision of the HYSPILT transport model and READY website
385 (http://www.arl.noaa.gov/ready.php) used in this paper.

386 **References**

387 Cao, J. J., Lee, S. C., Ho, K. F., Zhang, X. Y., Zou, S. C., Fung, K., Chow, J. C., Watson, J.
388 G., 2003. Characteristic of carbonaceous aerosol on Pearl River Delta region, China
389 during 2001 winter period. Atmoss Environ., 37, 1451-1460.
390 Cooke, W. F., Liousse, C., Cachier H., Feichter, J., 1999. Construction of a 1° x 1° fossil
391 fuel emission data set for carbonaceous aerosol and implementation and radiative impact
392 in the ECHAM4 model. J. Geophys. Res. 104, 22137-22162.
393 Deshmukh, D. K., Deb, M. K Suzuki, Y., Kouvarakis. G. N., 2013. Water-Soluble Ionic
394 Composition of $PM_{2.5–10}$ and $PM_{2.5}$ Aerosols in the Lower Troposphere of an Industrial
395 City Raipur, the Eastern Central India. Air Quality, Atmosphere and Health, Springer, 6:
396 95 - 110.
397 Duan, J., Tan, J., Yang, L., Wu, S., and Hao, J., 2008. Concentration, sources and ozone
398 formation potential of volatile organic compounds (VOCs) during ozone episode in
399 Beijing, Atmos. Res., 88, 25–35, 2008.
400 Fu, P. Q., et al., 2012. Diurnal variations of organic molecular tracers and stable carbon
401 isotopic compositions in atmospheric aerosols over Mt. Tai in the North China Plain: an
402 influence of biomass burning, Atmos. Chem. Phys., 12, 8359–8375.
403 Draxler, R. R., Hess, G. D., 1998. An overview of the HYSPLIT_4 modelling system for
404 trajectories, dispersion and deposition. Australian Meteorological Magazine 47, 295-308.
405 Fu, P., Kawamura, K., Usukura, K., Miura, K., 2013, Dicarboxylic acids, ketocarboxylic
406 acids and glyoxal in the marine aerosols collected during a round-the-world cruise.
407 Marine Chemistry, 148, 22–32.
408 Guo, H., Wang, T., Blake, D.R., Simpson, I.J., Kwok, Y.H., Li, Y.S., 2006. Regional and
409 local contributions to ambient non-methane volatile organic compounds at a polluted
410 rural/coastal site in Pearl River Delta, China, Atmos. Environ. 40, 2345–2359
411 Ho, K. F., Lee, S. C., Ho, S. S. H., Kawamura, K., Tachibana, E., Cheng, Y., and Zhu, T.,
412 2010, Dicarboxylic acids, ketocarboxylic acids, α-dicarbonyls, fatty acids and benzoic
413 acid in urban aerosols collected during 2006 Campaign of Air Quality Research in
414 Beijing (CAREBeijing-2006). J. Geophys. Res., 115, D19312, doi:1029/2009JD013304.
415 Ho, K. F., Lee, S. C., Cao, J. J., Kawamura, K., Watanabe, T., Cheng, Y., Chow, J. C., 2006.
416 Dicarboxylic acids, ketocarboxylic acids and dicarbonyls in the urban roadside area of
417 Hong Kong. Atmos. Environ. 40, 3030-3040.

Ho, K. F., Ho, S. S. H., Lee, S. C., Kawamura, K., Zou, S. C., Cao, J. J., Xu, H. M., 2011. Summer and winter variations of dicarboxylic acids, fatty acids and benzoic acid in $PM_{2.5}$ in Pearl Delta River Region, China. Atmos. Chem. Phys. 11, 2197-2208.

Jimenez, J. L., et al., 2009. Evolution of organic aerosols in the atmosphere, Science, 326, 1525-1529.

Kallinger, G., Niessner, R., 1999. Laboratory investigation of annular denuders as sampling system for the determination of aliphatic primary and secondary amines in stack gas. Mikrochimica Acta 130, 309–316.

Kanakidou, M., et al., 2005. Organic aerosol and global climate modelling: a review. Atmos. Chem. Phys. 5, 1053–1123, SRef-ID: 1680-7324/acp/2005-5-1053.

Kawamura, Ng, K., L. and Kaplan, I. R., 1985. Determination of organic acids (C_1-C_{10}) in the atmosphere, motor-exhausts and engine oils. Environ. Sci. and Technol. 19, 1082-1086.

Kawamura, K. and Gagosian, R. B., 1987. Implications of ω-oxocarboxylic acids in the remote marine atmosphere for photo-oxidation of unsaturated fatty acids. Nature 325, 330-332.

Kawamura, K., 1993. Identification of C_2-C_{10} ω-oxocarboxylic acids, pyruvic acid, and C_2-C_3 α-dicarbonyls in wet precipitation and aerosol samples by capillary GC and GC-MS, Anal. Chem., 65, 3505–3511.

Kawamura, K., Ikushima, K., 1993. Seasonal changes in the distribution of dicarboxylic acids in the urban atmosphere. Environ. Sci. Technol. 27, 2227-2235.

Kawamura, K., and F. Sakaguchi (1999), Molecular distributions of water soluble dicarboxylic acids in marine aerosols over the Pacific Ocean including tropic, J. Geophys. Res., 104, 3501-3509.

Kawamura, K., Kobayashi, M., Tsubonuma, N., Mochida, M., Watanabe, T., Lee, M., 2004. Organic and inorganic compositions of marine aerosols from East Asia: seasonal variations of water-soluble dicarboxylic acids, major ions, total carbon and nitrogen, and stable C and N isotopic composition. In: Hill, R.J., et al. (Eds.), Geochemical Investigations in Earth and Space Science: A Tribute to Isaac R. Kaplan. The Geochemical Society, Publication No. 9, pp. 243–265.

Kawamura, K., Kasukabe, H. and Barrie L. A. 2010. Secondary formation of water-soluble organic acids and α-dicarbonyls and their contribution to total carbon and water-soluble

organic carbon: Photochemical ageing of organic aerosols in the Arctic spring. J. Geophys. Res., 115, D21306, doi: 10. 1029/2010JD014299.

Kawamura, K. and Pavuluri, C. M., 2010. New Directions: Need for better understanding of plastic waste burning as inferred from high abundance of terephthalic acid in South Asian aerosols, Atoms. Environ., 44, 5320-5321.

Kolattukudy, P. E., 1976. Chemistry and Biochemistry of Natural Waxes; Elsevier: New York.

Kundu, S., Kawamura, K., Lee, M., 2010. Seasonal variations of diacids, ketoacids and α-dicarbonyls in marine aerosols at Gosan, Jeju Island: Implications for their formation and degradation during long-range transport. J. Geophys. Res. 115, D19307, doi: 10.1029/2010JD013973.

Kunwar, B., Kawamura, K., 2014a. One-year observations of carbonaceous and nitrogenous components and major ions in the aerosols from subtropical Okinawa Island, an outflow region of Asian dusts. Atmos. Chem. Phys. 14, 1819-1836, doi: 10.5194/acp-14-1819-2014.

Kunwar, B. and Kawamura, K. 2014b, Seasonal distributions and sources of low molecular weight dicarboxylic acids, ω-oxocarboxylic acids, pyruvic acid, α-dicarbonyls and fatty acids in ambient aerosols from subtropical Okinawa in the western Pacific rim. Environ. Chem., 108, 49-58, doi:10. 1071/EN14097.

Mace, K.A., Artaxo, P., Duce, R.A., 2003. Water-soluble organic nitrogen in Amazon Basin aerosols during the dry (biomass burning) and wet seasons. J. of Geophys. Res.-Atmospheres, 108, NO. D16, 4512, doi:10.1029/2003JD003557.

Mitchell, D. M., Solomon, M. A., Tolfree, S. E., Short, M., Spiro, S. G., 1987. Effect of particle size of bronchodilator aerosols on lung distribution and pulmonary function in patients with chronic asthma. Thorax., 42(6), 457–461.

Ohara, T., Akimoto, H., Kurokawa, J., Horii, N., Yamaji, K., Yan, X. and Hayasaka, T. 2007, An Asian emission inventory of anthropogenic emission sources for the period 1980-2020. Atmos. Chem. Phys., **7**, 4419-4444.

Pavuluri, C., M., Kawamura, K., Swaminathan, T., 2010. Water-soluble organic carbon, dicarboxylic acids, ketoacids, and α-dicarbonyls in the tropical Indian aerosols. J. Geophys. Res., 115, D11302, doi: 10.1029/ 2009JD012661.

Pavuluri, C., M., Kawamura, K., Swaminathan, T., 2015. Time-resolved distributions of bulk parameters, diacids, ketoacids and α-dicarbonyls and stable carbon and nitrogen

isotope ratios of TC and TN in tropical Indian aerosols: Influence of land/sea breeze and secondary processes, Atmos. Res., 153, 188–19

Ramanathan, V., Crutzen, P. J., Kiehl, J. T., Rosenfeld, D., 2001. Aerosols, climate, and the hydrological cycle, Science., 294, 2119– 2124.

Saltzman, E. S., D. L. Savoie, R. G. Zika, and J. M. Prospero (1983), Methane sulfonic acid in the marine atmosphere, J. Geophys. Res., 88(C15), 10897–10902, doi:10.1029/JC88iC15p10897.

Sang, X-F., et al., 2011. Levoglucosan enhancement in ambient aerosol during springtime transport events of biomass burning smoke to Southeast China, Tellus, 63B, 129-139.

Sato, K., Li, H., Tanaka, Y., Ogawa, S., Iwasaki, Y., Takami, A., Hatakeyama, S., 2009. Long-range transport of particulate polycyclic aromatic hydrocarbons at Cape Hedo remote island site in the East China Sea between 2005 and 2008. J. Atmos. Chem. 61, 243-257.

Simoneit, B. R. T., 1978. The organic chemistry of marine sediments. Chemical oceanography; Riley, J. P., Chester, R., Eds.; Academic Press: New York, Vol. 7.

Simoneit, B.R.T., Rushdi, A.I., bin Abas, M.R., Didyk, B.M., 2002. Alkyl amides and nitriles as novel tracers for biomass burning. Environmental Science & Technology 37, 16–21.

Simoneit, B.R.T., Medeiros, P.M., Didyk, B.M., 2005. Combustion products of plastics as indicators for refuse burning in the atmosphere. Environ. Sci. & Technol. 39, 6961-6970.

Sorooshian, A., et al., 2008. Comprehensive airborne characterization of aerosol from a major bovine source. Atmospheric Chemistry and Physics 8, 5489–5520.

Suh, I., Zhang, R., Molina, L. T., Molina, M. J., 2003. Oxidation mechanism of aromatic peroxy and bicyclic radicals from OH-toluene reactions. J. Amer. Chem. Soc. 125, 12655-12665.

Sempéré, R., Kawamura, K., 2003. Trans-hemispheric contribution of C_2-C_{10} α,ω-dicarboxylic acids, and related polar compounds to water-soluble organic carbon in the western Pacific aerosols in relation to photochemical oxidation reactions. Global Biogeochem. Cycles 17(2), 1069, doi: 10.1029/2002GB001980.

Takami, A., et al., 2007. Transport of anthropogenic aerosols from Asia and subsequent chemical transformation. *J. Geophys. Res.*, 112, D22S31, doi:10.1029/2006JD008120, 2007108:8425, doi:10.1029/2001JD001213.

515 Timperley, M.H., Vigor-Brown, R.J., Kawashima, M., Ishigami, M., 1985. Organic nitrogen
516 compounds in atmospheric precipitation:their chemistry and availability to phytoplankton.
517 Canadian Journal of Fisheries and Aquatic Sciences 42, 1171–1177.
518 Wang, G. H., Zhou, B. H., Cheng, C. L., Cao, J. J., Meng, J. J., Tao, J., Zhang, R. J., and Fu,
519 P. Q., 2013. Impact of Gobi desert dust on aerosol chemistry of Xi'an, inland China
520 during spring 2009: differences in composition and size distribution between the urban
521 ground surface and mountain atmosphere, Atoms. Chem. Phys., 13, 819-835, doi:
522 10.5194/acp-13-819-2013.
523 Wang, G., Kawamura, K., Umemoto, N., Xie, M., Hu, S., Wang, Z., 2009. Water-soluble
524 organic compounds in PM2.5 and size-segregated aerosols over Mount Tai in North
525 China Plain. J. Geophys. Res. 114, D19208, doi: 10.1029/ 2008JD011390.
526 Yamamoto, S. and Kawamura, K. 2010, Stable hydrogen isotopic compositions of fossil
527 fuel-derived n-alkanes in the atmospheric aerosols from Okinawa, Japan. Res. Org.
528 Geochem. 2011, 27, 81-89.
529 Simoneit, B.R.T., et al., 1999, Levoglucosan, a tracer for cellulose in biomass burning and
530 atmospheric particles, doi.org/10.1016/S1352-2310(98)00145-9.
531 Wedyan, M.A., Preston, M.R., 2008. The coupling of surface seawater organic nitrogen and
532 the marine aerosol as inferred from enantiomer-specific amino acid analysis. Atmos.
533 Environ. 42, 8698–8705
534 Westerholm, R., Li, H., Almén, J., 1993. Estimation of aliphatic amine emissions in
535 automobile exhausts. Chemosphere 27, 1381–1384.
536 Yuan Hui., Ying, Wang., Guoshum, Zhuang. 2004. MSA in Beijing aerosol, Chinese
537 Science Bulletin 2004, vol. 49, 10, 1020 -1025.
538 Zhu. C., Kawamura, K., Kunwar, B., 2015. Effect of biomass burning over western North
539 Pacific Rim: wintertime maxima of anhydrosugars in ambient aerosols from Okinawa.
540 Atoms. Chem. Phys., 15, 1959-1973, doi: 10.5194/acp-15-1959-2015.

541 Figure Captions

542 Figure 1. (a) 5-day backward trajectories during study period. Back trajectory analysis was
543 performed at 500 m above ground level with the NOAA HYSPLIT model. (b) 5-day backward
544 trajectories with fire counts for specific days.

545 Figure 2. Averaged molecular distributions of straight chain diacids (C_2 -C_{12}), branched chain
546 diacids (iC_4- iC_6), unsaturated diacids (M, F, mM, Ph, iPh, and tPh), multifunctional diacids
547 (hC_4, kC_3 and kC_7), oxoacids (ωC_2-ωC_9, and pyruvic), and α-dicarbonyls (Gly and MeGly) in
548 $PM_{1.0}$ aerosols collected at Cape Hedo. The error bars represent the standard deviation.

549 Figure 3. Temporal variations of (a) oxalic acid (C_2), (b) malonic acid (C_3), (c) succinic acid (C_4),
550 (d) adipic acid (C_6), (e) azelaic acid (C_9), and (f) phthalic acid (Ph), (g) glyoxylic acid (ωC_2),
551 (h) 4-oxobutanoic acid (ωC_4), (i) 9-oxononanoic acid (ωC_9), (j) glyoxal (Gly), (k)
552 methylglyoxal (MeGly), and (l) benzoic acid in $PM_{1.0}$ aerosols collected at Cape Hedo,
553 Okinawa.

554 Figure 4. Temporal variations in the concentration ratios of (a) malonic/succinic (C_3/C_4), (b)
555 adipic/azelaic (C_6/C_9), (c) phthalic/azelaic (Ph/C_9), and (d) fumaric/maleic (F/M) acids in
556 $PM_{1.0}$ aerosols collected at Cape Hedo, Okinawa.

557 Figure 5. Temporal variations of (a) organic carbon (OC) and elemental carbon (EC), (b) organic
558 nitrogen (ON), (c) NH_4^+, (d) nss-SO_4^{2-}, (e) MSA^-, (f) nss-K^+, and (g) levoglucosan in $PM_{1.0}$
559 aerosols collected at Cape Hedo, Okinawa.

560 Figure 6. Scatterplot between (a) OC and EC, and (b) SO_4^{2-} and NH_4^+ in aerosols collected from
561 Cape Hedo, Okinawa.

562 Figure 7. Scatterplot between total nitrogen (TN) and NH_4-N+NO_3-N in aerosols collected from
563 Cape Hedo, Okinawa.

564 Figure 8. Scatterplots between (a) NH_4^+ and total diacids, (b) SO_4^{2-} and total diacids, (c) MSA^- and
565 total diacids, and (d) Na^+ and total diacids in aerosols collected from Cape Hedo, Okinawa.

566 Figure 9. Averaged molecular distributions of fatty acids in $PM_{1.0}$ aerosols collected from Cape
567 Hedo, Okinawa. The first number of fatty acid indicates the carbon numbers whereas the
568 second number indicates the number of double bond.

569

570

571

572 Table 1. Concentrations of diacids and related compounds in atmospheric aerosols from
573 Cape Hedo, Okinawa (2007 spring).

	Concentrations (ng m^{-3})	
Species	AV±SD	Range
	Diacids	
Oxalic, C_2	172±73	78-329
Malonic, C_3	26±13	7.5-58
Succinic, C_4	20±11	5.2-53
Glutaric, C_5	4.5±2.5	1.0-9.9
Adipic, C_6	2.9±2.0	0.31-9.3
Pimeric, C_7	0.60±0.71	BDL-3.1
Suberic, C_8	0.93±2.2	BDL-11
Azelaic,C_9	3.3±0.75	0.37-4.5
Sebacic, C_{10}	0.39±0.37	BDL-1.2
Dodecanedioic, C_{12}	0.91±0.43	0.32-1.9
Methylmalonic, iC_4	4.3±2.5	1.3-9.8
Methylsuccinic, iC_5	1.2±0.91	0.17-3.1
Methylglutaric, iC_6	0.36±0.26	BDL-0.95
Maleic, M	1.6±1.0	0.33-4.9
Fumaric, F	0.68±0.47	0.20-2.2
Methylmaleic, mM	2.0±3.9	BDL-11
Phthalic, Ph	12±8.4	2.39-35
Isophthalic, iPh	0.74±0.63	0.04-2.2
Terephthalic, tPh	0.22±2.2	BDL-7.2
Hydroxysuccinic, hC_4	0.21±0.15	0.07-0.87
Ketomalonic, kC_3	15±14	0.45-69
Ketopimelic, kC_7	3.4±2.0	0.61-7.8
Total diacids	273±121	114-537
	Oxoacids	
Glyoxylic, ωC_2	22±12	4.7-44
3-Oxopropanoic, ωC_3	0.02±0.04	BDL-0.14
4-Oxobutanoic ωC_4	2.9±2.0	0.15-7.32
9-Oxononoic, ωC_9	2.2±1.3	0.46-6.2
Total oxoacids	27±15	5.5-53
Pyruvic acid	4.9±2.5	1.7-10
Benzoic acid	17±9.2	4.3-36
	α-Dicarbonyls	
Glyoxal, Gly	2.9±2.3	0.44-9.0
Methylglyoxal, MeGly	4.9±2.0	2.0-9.6
Total α-dicabonyls	7.8±4.2	2.9-18

574 Note: BDL means below detection limit (<0.001 ng m^{-3})

575

576 Table 2: Correlation (r) analyses among diacids species and selected major ions in aerosols from Cape Hedo, Okinawa, Japan.

	C_2	C_3	C_4	C_6	C_7	C_9	Ph	ωC_2	ωC_9	Pyr	Na^+	$nssK^+$	NO_3^-	$nssSO_4^{2-}$	MSA^-	Levo
C_2	1.00															
C_3	**0.94**	1.00														
C_4	**0.90**	**0.95**	1.00													
C_6	0.58	0.63	0.62	1.00												
C_7	0.44	0.49	0.50	**0.86**	1.00											
C_9	0.19	0.11	0.14	0.32	0.32	1.00										
Ph	0.42	0.46	**0.65**	**0.61**	0.57	0.31	1.00									
ωC_2	**0.83**	**0.89**	**0.87**	**0.70**	0.55	0.35	0.62	1.00								
ωC_9	**0.81**	**0.90**	**0.86**	0.47	0.33	0.10	0.36	**0.78**	1.00							
Pyr	**0.73**	**0.86**	**0.81**	**0.69**	**0.61**	0.27	0.62	**0.93**	0.78	1.00						
Na^+	-0.02	0.10	0.17	-0.07	-0.02	-0.17	0.00	-0.02	0.20	0.08	1.00					
$nssK^+$	0.57	0.61	0.54	0.33	0.36	0.26	0.28	0.58	0.45	0.43	-0.17	1.00				
NO_3^-	-0.10	-0.25	-0.26	-0.19	-0.13	-0.04	-0.16	-0.27	-0.27	-0.27	-0.09	-0.22	1.00			
$nssSO_4^{2-}$	**0.81**	**0.85**	**0.84**	0.55	0.45	0.42	0.45	**0.85**	0.81	**0.75**	0.10	**0.69**	-0.29	1.00		
MSA^-	**0.82**	**0.80**	**0.86**	0.56	0.43	0.21	0.52	**0.74**	**0.72**	0.64	0.16	0.47	-0.14	**0.84**	1.00	
Levo	0.46	0.52	0.46	**0.64**	**0.60**	0.33	0.50	**0.76**	0.32	**0.71**	-0.27	0.44	-0.20	0.49	0.38	1.00

577
578

Table 3. Principal component analysis of selected diacids, oxoacid and major ions in the aerosols from Cape Hedo, Okinawa.

	Component			
Species	1	2	3	4
C_2	**0.94**	0.14	0.09	-0.03
C_3	**0.94**	0.22	0.08	-0.12
C_4	**0.91**	0.30	0.05	-0.12
C_5	**0.83**	0.30	0.28	-0.04
C_6	0.44	**0.79**	0.31	-0.01
C_7	0.30	**0.79**	0.35	-0.03
C_8	0.03	**0.92**	-0.12	-0.07
C_9	0.04	0.10	**0.79**	-0.04
Ph	0.38	0.58	0.31	0.02
ωC_2	**0.82**	0.24	0.43	-0.09
Na^+	-0.27	0.09	-0.01	**0.88**
NH_4^+	**0.90**	0.12	0.18	-0.24
$nssK^+$	0.61	-0.02	0.34	-0.27
NO_3^-	-0.08	-0.15	-0.06	**0.91**
$nssSO_4^{2-}$	**0.90**	0.15	0.17	-0.22
MSA^-	**0.85**	0.28	0.00	-0.04
levo	0.41	0.28	**0.69**	-0.00
Variance	54%	13%	9%	7%

591 Figure

592 1

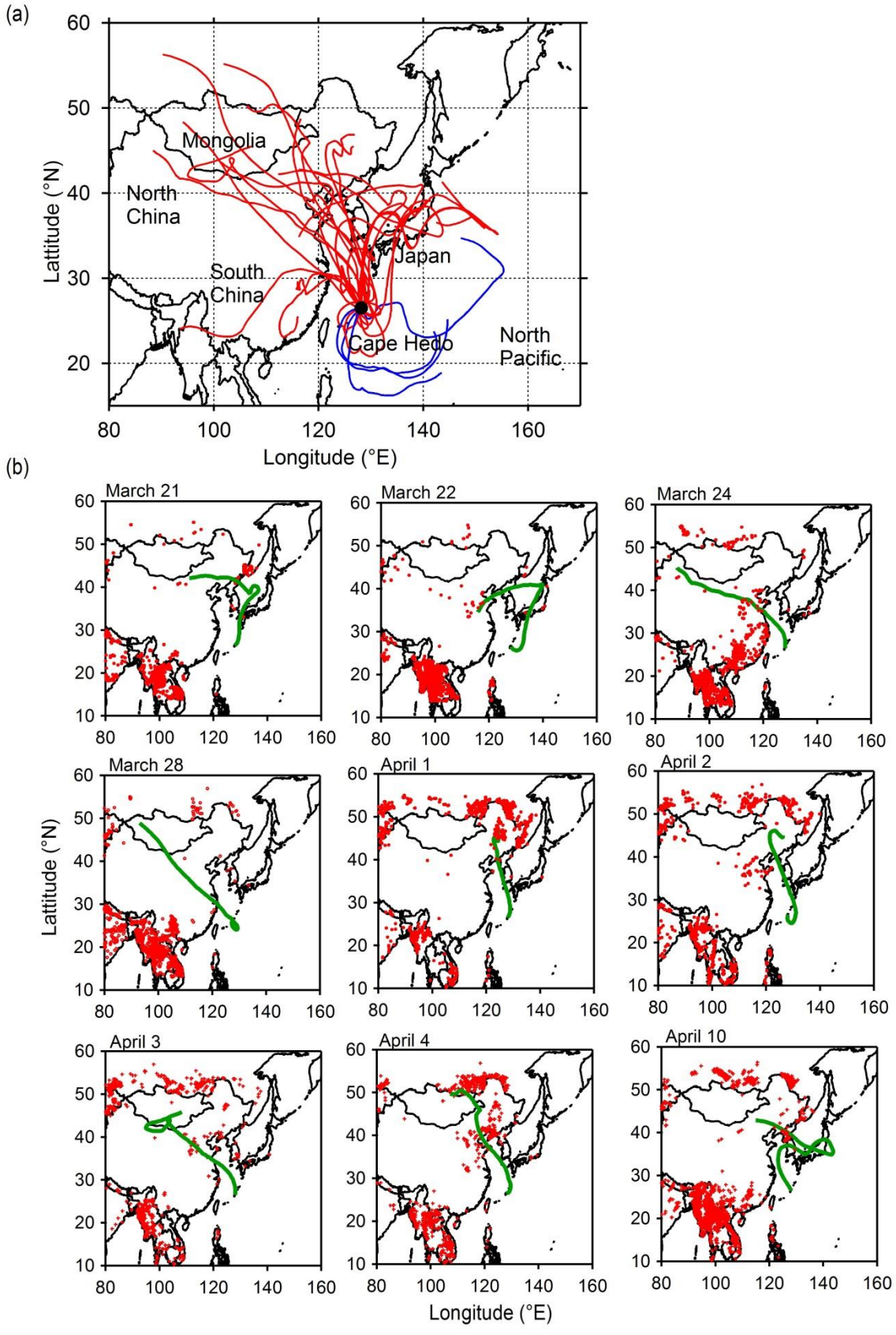

593

Figure 2

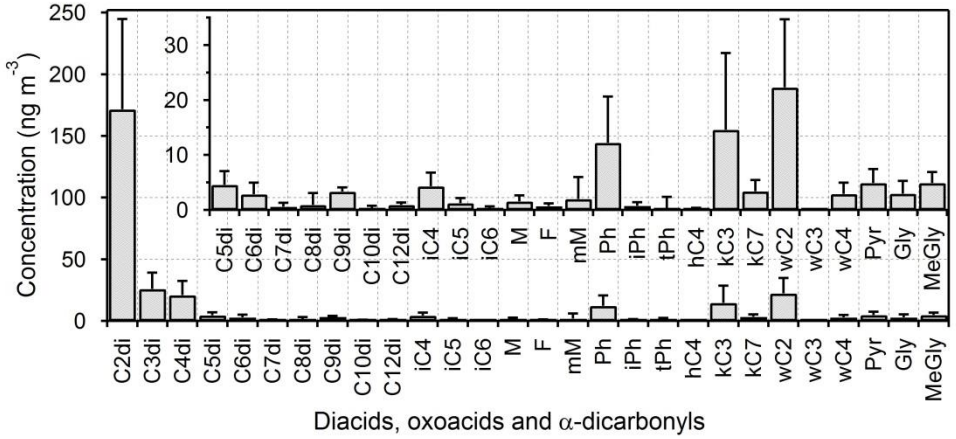

Figure 3

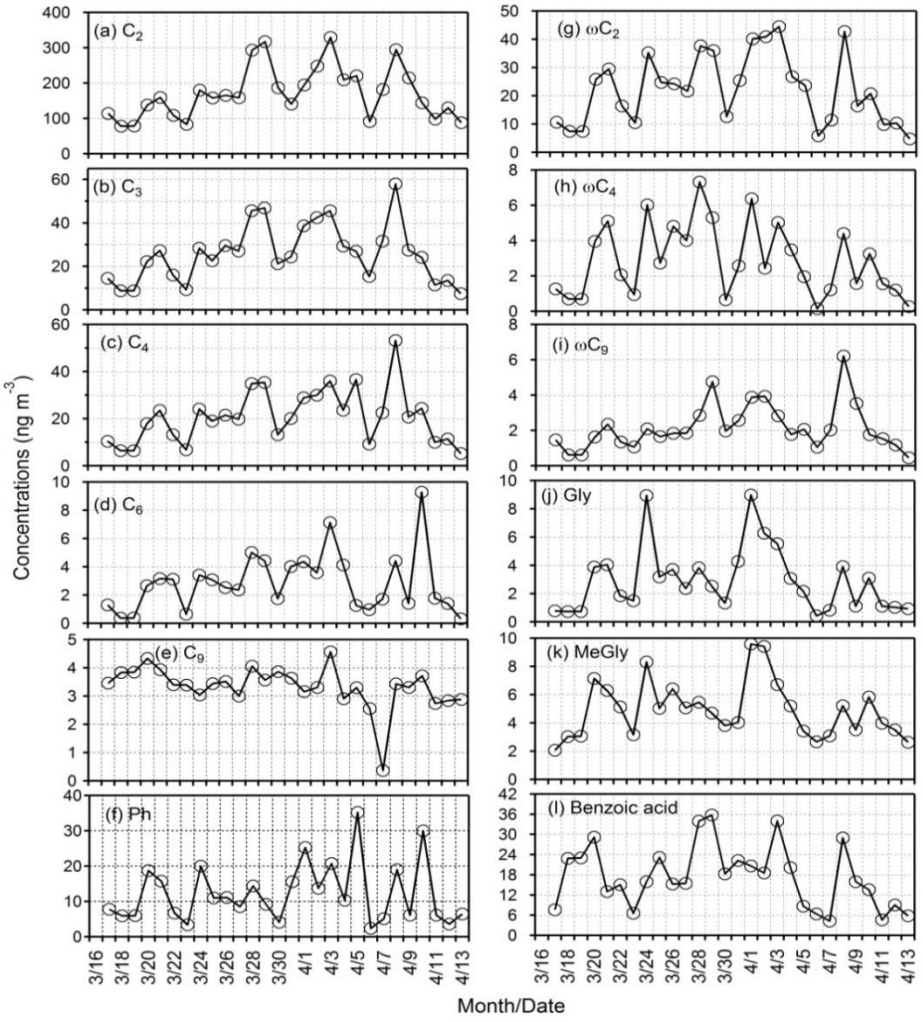

598 Figure 4

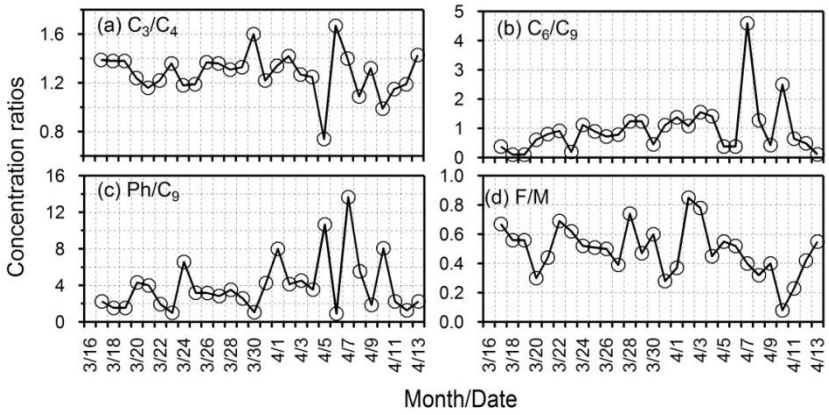

599

600

601

602

603

604

605

606

607

608

609

610

611

612

613 Figure 5

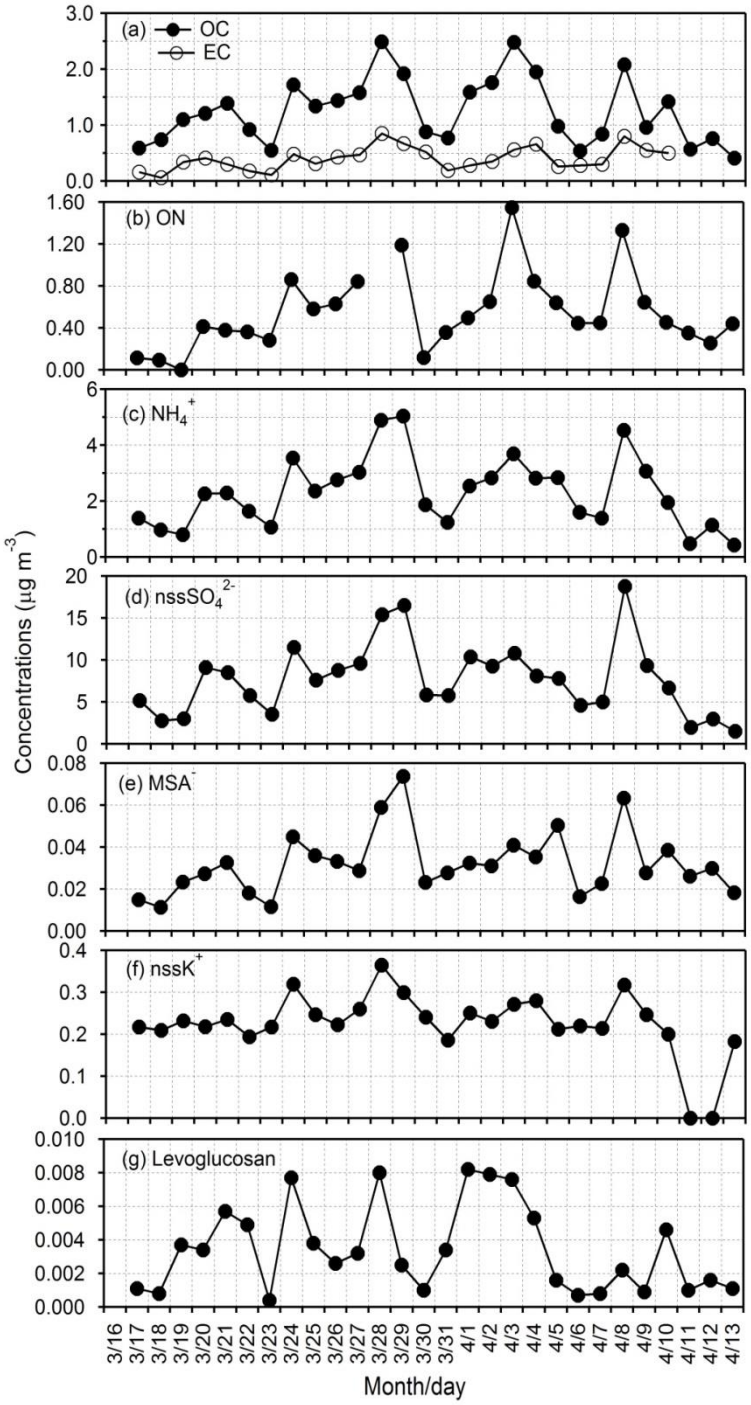

614

615

616

617

618 Figure 6a

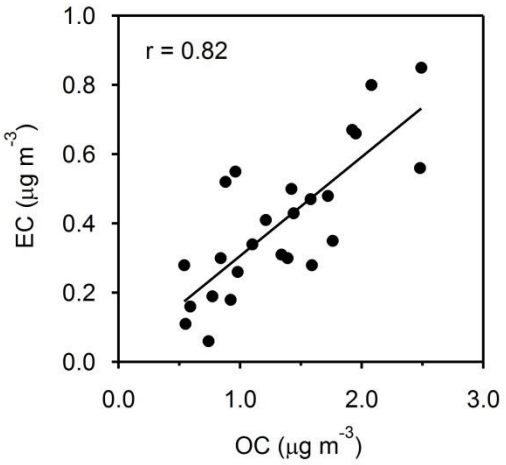

619

620 Figure 6b

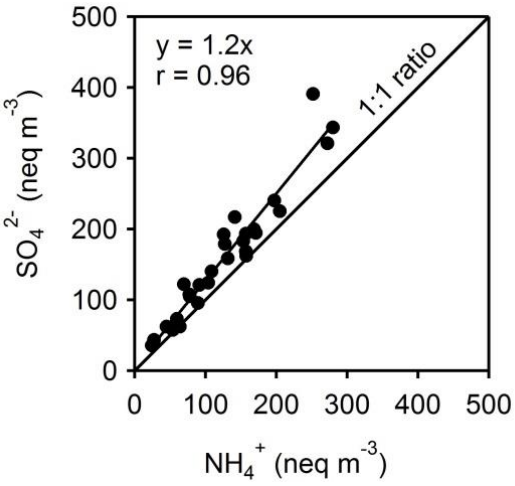

621

622 Figure 7

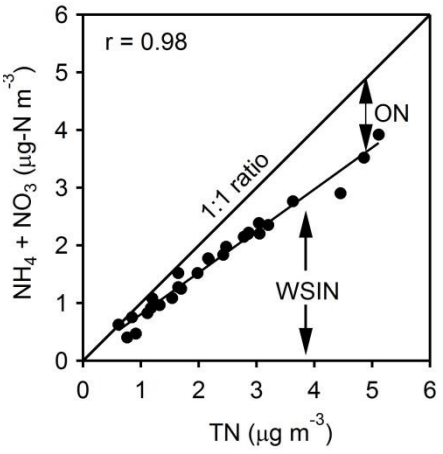

623

624 Figure 8

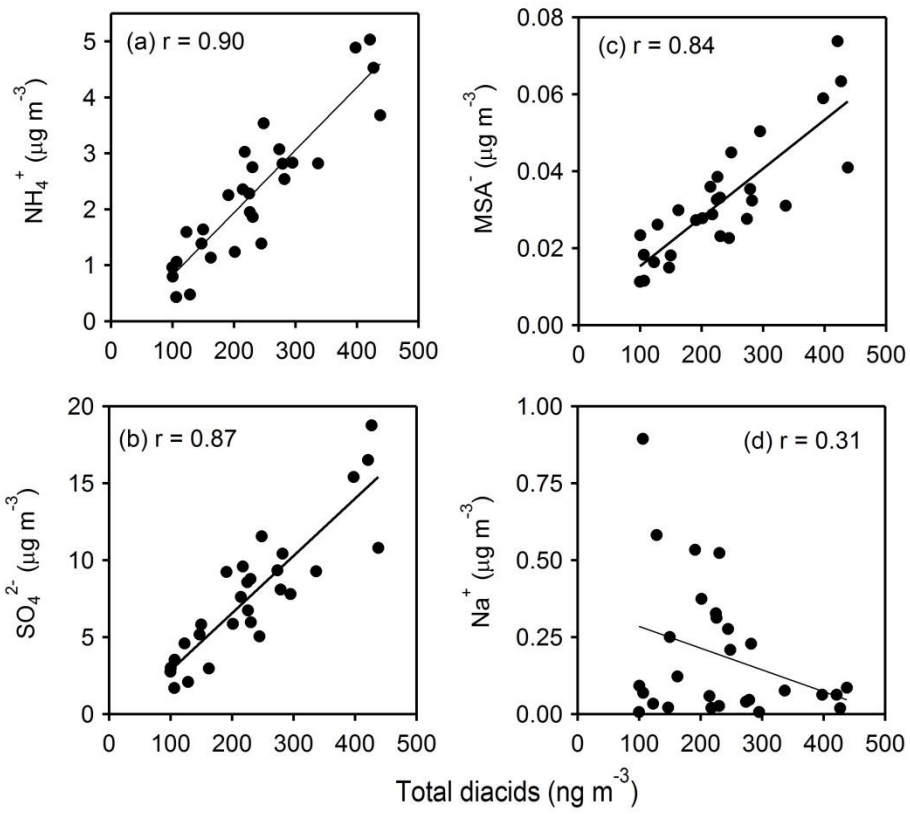

625

626 Figure 9

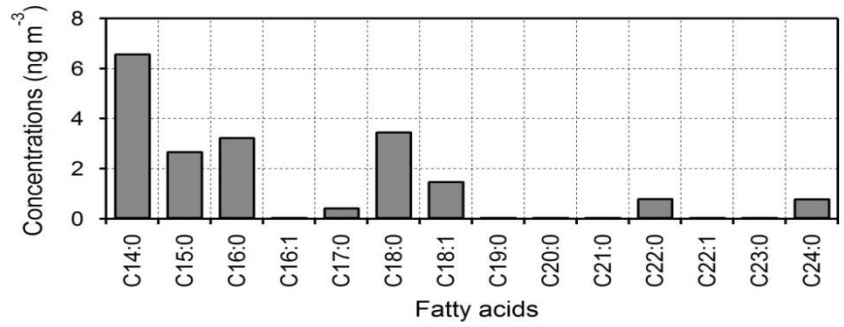

627

628

629

630

631 Supporting Information

632 Figure S1.A geographical map of sampling location, Cape Hedo, Okinawa, Japan.

633 Figure S2. Temporal variations of (a) rain fall (b) temperature and (c) relative humidity recorded in
634 Cape Hedo, Okinawa.

635

636 Figure S1.

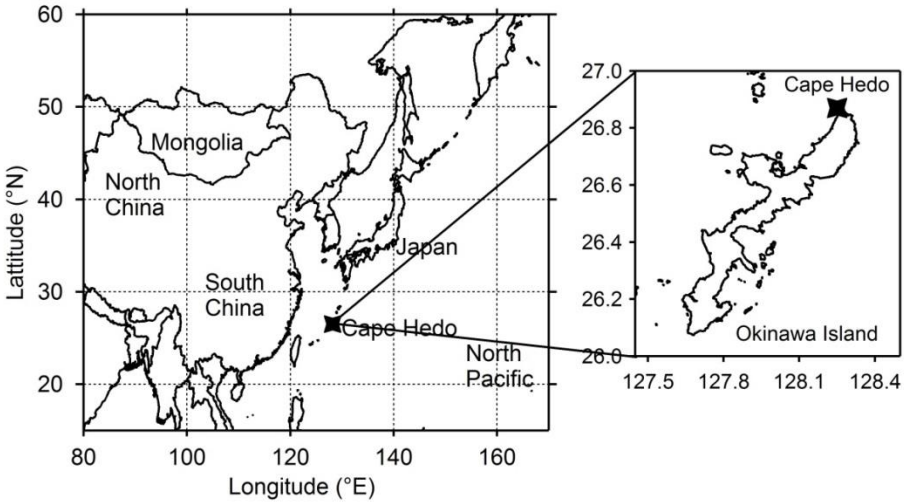

637

638 Figure S2.

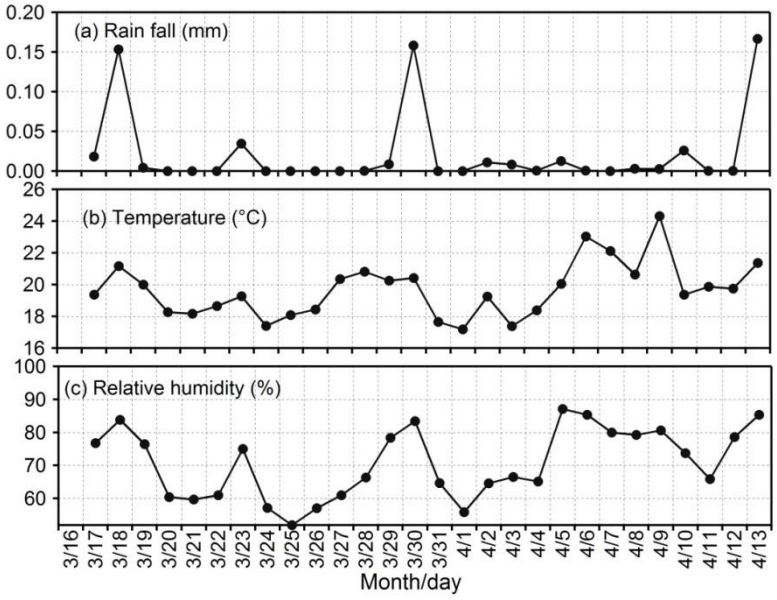

639

640